



Influence of deposition temperature on the structure of 3,4,9,10-perylene tetracarboxylic dianhydride thin films on H-passivated silicon probed by Raman spectroscopy

G. Salvan^a, D.A. Tenne^{a,b}, A. Das^c, T.U. Kampen^a, D.R.T. Zahn^{a,*}

^a *Institut für Halbleiterphysik, Technische Universität Chemnitz, D-09107 Chemnitz, Germany*

^b *Institute of Semiconductor Physics, 630090 Novosibirsk, Russia*

^c *Materials Science Division, Indira Gandhi Centre for Atomic Research, Kalpakkam 603 102, Tamil Nadu, India*

Received 27 April 2000; received in revised form 7 July 2000; accepted 7 July 2000

Abstract

Raman spectroscopy was used to characterize the structural order in thin organic films of 3,4,9,10-perylene tetracarboxylic dianhydride (PTCDA). Films of the same average thickness were grown by organic molecular beam deposition on hydrogen-passivated p-type silicon (100) substrates at different growth temperatures between 230 and 470 K. The Raman spectra of all samples exhibit four external vibrational modes, that occur as a consequence of the arrangement of the PTCDA molecules in a crystalline environment. The full width at half maximum of these phonon lines decreases with increasing temperature of the substrate during deposition. A similar tendency is also observed for the Raman-active internal molecular modes. In addition, with increasing deposition temperature the diffusely scattered light background in the Raman spectra increases, as well as the photoluminescence background in the high frequency range. We relate the observed spectral changes to an increase in the size of the crystalline domains within the films with increasing deposition temperature, an effect that is macroscopically reflected by an enhanced degree of surface roughness. The different quality of the crystalline PTCDA domains was also complementary revealed by X-ray diffraction measurements. © 2000 Elsevier Science B.V. All rights reserved.

PACS: 78.66.Qn; 78.70.Ck

Keywords: 3,4,9,10-Perylene tetracarboxylic dianhydride; Silicon; Vibrations; Raman spectroscopy; X-ray diffraction

1. Introduction

Thin films of organic semiconductors have already proved a great potential for optoelectronic devices [1]. Progress has greatly benefited from

controlled film deposition under clean ultra-high vacuum (UHV) conditions: organic molecular beam deposition (OMBD). Additional potential for future applications lies in combining organic and inorganic semiconductors for electronic devices. Device performance will markedly be influenced by the degree of structural order in the organic films which to a large extent controls the electronic properties (such as carrier mobilities) as well as the optical ones. The structural order itself

* Corresponding author. Tel.: +49-371-5313036; fax: +49-371-5313060.

E-mail address: zahn@physik.tu-chemnitz.de (D.R.T. Zahn).

is expected to depend critically on the growth parameters, in particular on the substrate temperature.

The film formation properties of the archetype organic molecule 3,4,9,10-perylene tetracarboxylic dianhydride (PTCDA) on a variety of inorganic substrates have already been studied by a number of experimental and theoretical methods [1–4]. The most commonly used substrate materials have been weakly interacting ones, such as metals (e.g. Ag and Au), highly oriented pyrolytic graphite, and insulators (NaCl, SiO₂, Al₂O₃) [1], while investigations using the more reactive surfaces of more common inorganic semiconductors such as silicon and gallium arsenide have been scarce.

On clean GaAs(1 0 0) [5] or Si(1 0 0) [6] surfaces a strong chemical interaction occurs between the anhydride groups of the molecules at the interface and the substrate, predominantly with the dangling bonds and defects. This usually results in the formation of small crystalline domains, in nearly random azimuthal orientation. Improved structural order is observed when reactive semiconductor substrate surfaces are passivated, e.g. by reaction with chalcogen or hydrogen atoms in the case of GaAs and Si substrates, respectively. The passivation induces a reduction of chemically active sites mainly by saturating dangling bonds [7]. Hence the work to be presented here concentrates on the deposition of PTCDA on hydrogen terminated Si(1 0 0), for the latter see [8]. Substrate temperature is a further important parameter that can control structural order. It was indeed already observed by X-ray diffraction (XRD) that the crystallite size drastically increased as temperature was raised from 320 to 370 K [9] when PTCDA was deposited on Si(1 0 0) wafers with natural oxide.

We have previously demonstrated that Raman spectroscopy is a versatile tool to characterize PTCDA films [10,11]. Raman spectra provide information on the internal vibrational modes of PTCDA molecules as well as on external vibrational modes (phonons). The latter were detected for all films deposited on passivated semiconductor substrates at frequencies between 40 and 125 cm⁻¹. These Raman active modes are of rotational–vibrational (libronic) origin in the PTCDA molecular crystal which has monoclinic symmetry

(space group C_{2h}⁵) with two molecules per unit cell (for a detailed discussion see [12]).

The first Raman study of the influence of substrate temperature on the growth process of PTCDA films on hydrogen-passivated (H-passivated) (100) oriented silicon surfaces to be reported here, reveals marked changes in the PTCDA phonon spectra. These changes can be correlated with the degree of structural order using additional XRD data.

2. Experimental

PTCDA films were grown on p-type (100) oriented silicon substrates by OMBD. The organic source material purchased from Lancaster was purified twice by sublimation at 575 K under high vacuum (10⁻⁶ Pa). To clean and passivate the surface, substrates were wet-chemically treated under atmospheric conditions. The first step of the chemical treatment consists of a 2 min etching in hydrofluoric acid (HF, 40%) to remove the silicon oxide and the organic contaminants, and thereafter H-passivate the dangling bonds on the surface. Secondly, rinsing in a buffered solution (HF + NH₄OH + NH₄F, pH 8) reduces the density of steps formed during the first processing stage [7]. The substrates were subsequently transferred into a UHV growth chamber with a base pressure below 2 × 10⁻⁸ Pa. Low energy electron diffraction (LEED) showed a sharp 1 × 1 diffraction pattern of the H-passivated Si(1 0 0) surface. Additionally, Auger electron spectroscopy (AES) revealed no oxygen signal and a silicon to carbon peak intensity ratio of ~37 corresponding to the absence of oxygen on the surface and to less than 10% of a monolayer of carbon contamination, respectively.

To determine the influence of the substrate temperature on crystalline growth, a series of PTCDA samples of approximately the same film thickness (~40 nm) was prepared at 230, 295, 360, 410 and 470 K. The substrate temperature was derived from the experimentally determined Raman shift of the Si phonon (2.2 cm⁻¹ per 100 K) which is linear in the relevant temperature range. The evaporation rate of PTCDA from the Knud-

sen cell was kept constant in all experiments by controlling the temperature to a value (550 K) that ensured a deposition rate of 3 \AA min^{-1} at room temperature (RT). Growth was interrupted when the monitored Raman signals of PTCDA and Si had the same intensity ratio as that obtained for a 40 nm thick PTCDA film grown at RT. The thickness of the latter was obtained from an atomic force microscopy calibration.

The UHV growth chamber is integrated into a macro-Raman configuration, that allows to perform in situ measurements in a backscattering geometry [13]. A lens of a focal length of 30 cm focuses the laser light onto the sample to a spot of about 300 μm in diameter. The scattered light is collected by a Dilor XY triple monochromator with a multi-channel charge coupled device detector. The Raman spectra were excited with the 488 nm (2.54 eV) Ar^+ laser line. The spectral resolution of the equipment was determined from the full width at half maximum (FWHM) of the laser line as $\sim 3.4 \text{ cm}^{-1}$. The laser power at the entrance of the UHV chamber was set to 20 mW, which limited the intensity of the focus to well below the damage threshold of PTCDA (at $\sim 100 \text{ kW cm}^{-2}$). For recording a spectrum 60 accumulations of 60 s each were used.

X-ray spectra were recorded ex situ using a SEIFERT 3000 PTS diffractometer with $\text{CuK}\alpha$ radiation ($\lambda = 1.5418 \text{ \AA}$). The measurements were performed in a $\theta - 2\theta$ scan mode in the range from 5° to 80° . Both Raman and XRD spectra were recorded at RT.

3. Results

The PTCDA evaporation rate used in our experiments leads to film deposition only when the substrate temperature is below 470 K. The film colour varied from bluish green for the sample grown at 230 K to reddish brown for that at 410 K. The film topography observed with an Olympus Microscope (objective magnification 100) was mirror-like for the films grown on substrates at RT and below, but for elevated temperatures a granular structure occurred. A similar observation was

already reported by Fughigami et al. for films deposited on gold (Au) substrates [14].

For films grown at 230, 295, 360 and 410 K (Fig. 1) the changes in morphology correlate with the differences we observe in the Raman spectra. Four bands below 100 cm^{-1} occur with all samples. These modes were recently attributed to external vibrational modes (phonons) of rotational (libronic) character [12] of the monoclinic PTCDA molecular crystal. Their frequency positions correspond well to those experimentally determined by Tenne et al. for PTCDA films deposited on $\text{Si}(111)\text{-H}:1 \times 1$ [12]. These modes are centred at 44, 65, 74 and 90 cm^{-1} and their symmetry is described by the A_g , B_g , A_g and B_g irreducible representations, respectively, of the C_{2h}^5 space group. The inset in Fig. 1 reveals a sharpening of the phonon bands with increasing temperature. This is more clearly seen after subtracting the background (Fig. 2). As an example, in the case of the mode at $\sim 44 \text{ cm}^{-1}$, which is most suited due to the absence of overlapping features, the FWHM has values of 12.5, 12, 10.2 and 8 cm^{-1} (within an accuracy of $\pm 0.4 \text{ cm}^{-1}$) for the samples grown at 230, 295, 360 and 410 K, respectively.

The Ar^+ laser line used for excitation, 2.54 eV, has an energy larger than the optical HOMO–LUMO gap (2.21 eV), and hence provides favourable conditions for resonance enhancement [15,16] of the Raman intensity. As the PTCDA molecule belongs to the D_{2h} symmetry point group, symmetry considerations dictate that the A_g symmetric internal vibrational modes dominate the spectra of isolated PTCDA molecules for the excitation energy used [17]. Density functional tight-binding calculations of the PTCDA molecular dynamics show that the lowest frequency internal mode ($\sim 233 \text{ cm}^{-1}$) mainly contains a contribution from the vibration of C–O bonds. The most intensive Raman lines at about 1303 and 1380 cm^{-1} correspond to modes with dominant C–H character. The mode at 1303 cm^{-1} has a large contribution of in-plane bending vibrations, while for the 1380 cm^{-1} mode the contribution of stretching vibrations is increased and the frequency of this mode is therefore higher. The two strong peaks at 1570 and 1589 cm^{-1} are assigned to modes with a dominant contribution of C–C

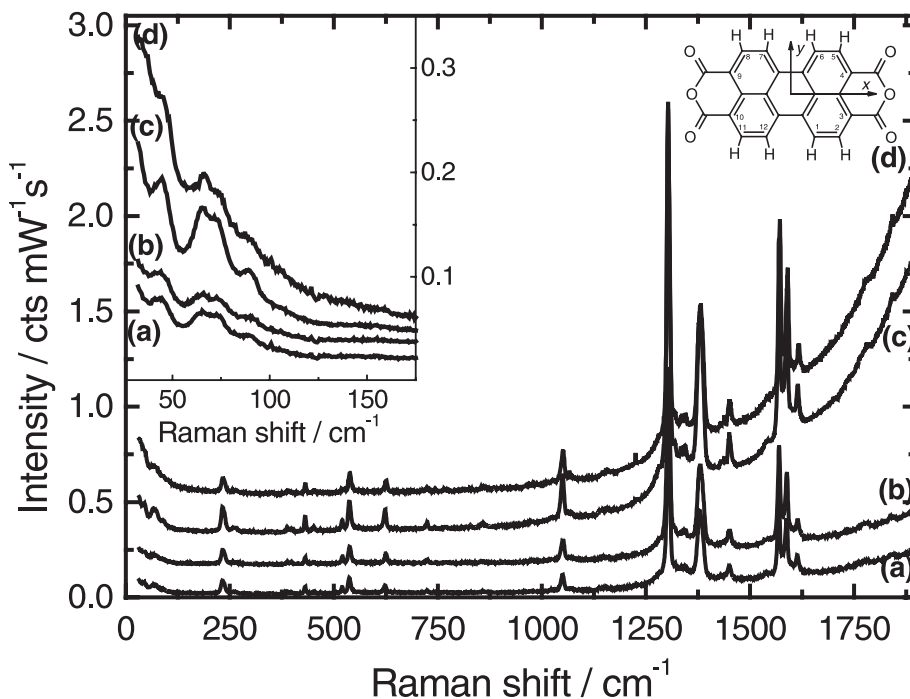


Fig. 1. Raman spectra of PTCDA films deposited on p-Si(100) substrates at the temperatures (a) 230 K, (b) 295 K, (c) 360 K and (d) 410 K. The left-hand inset shows the narrowing of the phonon lines below 125 cm^{-1} with increasing substrate temperature. The intensity units give the number of CCD counts divided by the total accumulation time and the incident laser power. The right-hand inset schematically presents the planar molecule PTCDA, $\text{C}_{24}\text{H}_8\text{O}_6$.

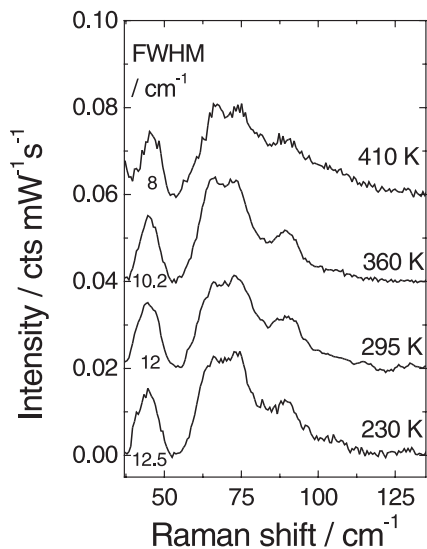


Fig. 2. Raman spectra of external vibrations (phonons) of PTCDA films obtained after the subtraction of a diffusely scattered light background. Spectra were normalized for a better comparison of the FWHM.

vibrations located at the perylene core. A weak and broad feature due to C=O vibrations appears at about 1780 cm^{-1} . The relative intensities of the Raman lines caused by scattering at internal vibrational modes are similar for all the films presented here. Frequency positions agree well with those of crystalline PTCDA [12].

FWHM of all the internal vibrational lines, except for the one at 233 cm^{-1} decreases with increasing temperature. In the case of the most prominent Raman mode at 1303 cm^{-1} (Fig. 3(a)), the FWHM for the samples grown at 230, 295, 360 and 410 K amounts to 11, 10.8, 10.1 and 8.8 cm^{-1} ($\pm 0.4\text{ cm}^{-1}$), respectively. Moreover, the shape of this line becomes asymmetric with increasing temperature, thus giving a hint for a double-peak structure.

Returning to Fig. 1, one notices that the background below 150 cm^{-1} and above 1600 cm^{-1} increases with the growth temperature. The background in the low frequency range originates

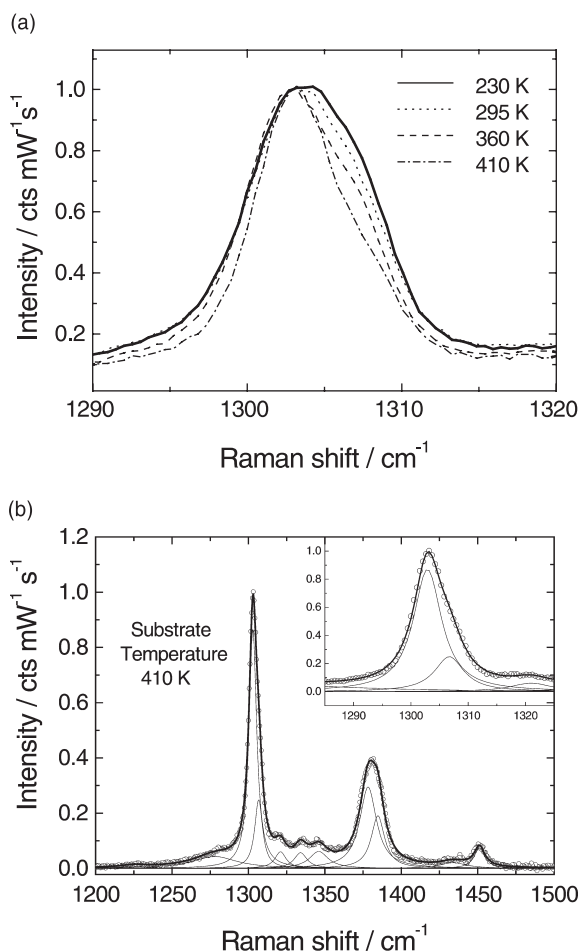


Fig. 3. (a) Normalized Raman spectra of the most prominent internal mode at $\sim 1303 \text{ cm}^{-1}$. The solid, dotted, dashed and dash-dotted curves in (b) correspond to the films grown at 230, 295, 360 and 410 K, respectively. (b) Multi-Lorentzian fit for the normalized Raman spectrum of the sample deposited at 410 K. A zoom of the region neighbouring the mode at $\sim 1303 \text{ cm}^{-1}$ is presented in the inset.

from diffusely scattered light, while in the high frequency range it presents a tail of the PTCDA photoluminescence.

The results obtained in Raman spectroscopy are closely correlated with the XRD spectra presented in Fig. 4. The films grown at 360 K and below show a diffraction peak around $2\theta \approx 27.62^\circ$. A Gaussian fit reveals that the angle corresponding to the diffraction maximum rises by 0.1° for the sample grown at 410 K. The FWHM of this peak

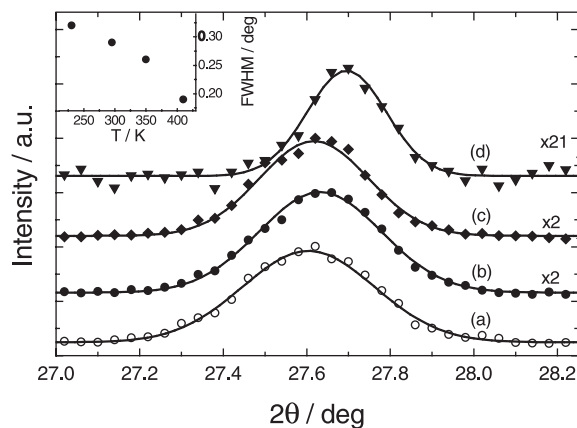


Fig. 4. XRD spectra of PTCDA films deposited on p-Si(100) substrates at temperatures (a) 230 K, (b) 295 K, (c) 360 K and (d) 410 K. The spectra were multiplied by the shown factors for better comparison. The curves represent a Gaussian fit to the experimental data (\blacktriangledown , \blacklozenge , \bullet , \circ).

decreases from 0.32° for the sample grown at 230 K to $0.19^\circ (\pm 0.02^\circ)$ for the sample deposited at 410 K. The latter value approaches that of 0.17° , obtained for a PTCDA crystal [12]. The peak narrowing effect is accompanied by a strong decrease of peak intensity for the highest substrate temperature.

4. Discussion

4.1. Raman spectroscopy

In Section 3 we have described the differences observed in the Raman spectra for PTCDA films deposited at various substrate temperatures. These results will be related in this section to a structural model.

Using LEED, AES and total current spectroscopy we have recently observed that PTCDA forms islands on H-passivated Si(111) substrates [18] when deposited at RT. Assuming the same growth mode for PTCDA on Si(100), the presence of the PTCDA phonon bands in the Raman spectra reveal the crystalline structure of domains within the films. Interestingly, the increase of growth temperature is accompanied by a decrease

of the FWHM of the phonon modes. To our knowledge, such an effect was not yet experimentally observed for molecular systems. Also, theoretical work applicable to this case is still lacking. We propose that the correlation between the FWHM of phonon bands and the structural order is similar to that observed in the case of inorganic semiconductor systems, such as gallium arsenide [21], carbon films [22] or germanium films [23]. There, the decrease in the FWHM of the optical phonon bands is related to the structural improvements induced by the growth or annealing temperature, i.e. to the development of the larger and more perfect single crystalline domains at the expense of the amorphous and polycrystalline contributions.

A small size of crystalline domains may affect both the phonon lifetime and the quasi-momentum conservation in the scattering process, and thus result in a broadening of the Raman phonon bands. However, a more quantitative evaluation of the FWHM would require a more detailed knowledge of phonon lifetime and dispersion curves in molecular crystals. In addition, the band broadening mechanism may also stem from the coexistence of crystalline domains consisting of α - and β -phase PTCDA.

Considering the internal modes, the mechanism that leads to the observed asymmetric narrowing provides further insight in the molecular crystal structure. We will concentrate our discussion on the mode at $\sim 1303\text{ cm}^{-1}$ shown in Fig. 3(a). It may seem, at the first glance, that the total decrease in the FWHM seen in Fig. 3(a) can be caused by an increased size of crystalline domains. However, the asymmetric shape that becomes more pronounced with increasing temperature is most likely to originate from a multi-component structure. A multi-Lorentzian fitting procedure, performed in the range between 1185 and 1500 cm^{-1} (Fig. 3(b)), reveals that the feature at $\sim 1303\text{ cm}^{-1}$ actually consists of two lines centred at 1302.9 and 1306.7 cm^{-1} ($\pm 0.2\text{ cm}^{-1}$). The fit also shows that the FWHM of the lower frequency component decreases from 7.9 to 6 cm^{-1} while the FWHM of the higher frequency component slightly increases from 5.4 to 6.2 cm^{-1} with increasing substrate temperature from 230 to 410 K . The splitting value

in the frequency positions of the doublet components amounts to 3.8 cm^{-1} for the PTCDA films and is larger than the value of the Davydov splitting (see below) of 1.7 cm^{-1} experimentally determined for a α -PTCDA crystal [12]. Raman data for the β -PTCDA crystals are not reported up to date.

One has to take into account that the crystalline environment causes a shift of each A_g internal mode of the isolated PTCDA molecule. This static field effect is stronger in the case of the α -PTCDA phase, where the molecules are more closely packed than in β -phase [1,24]. Hence, the vibrational frequency of internal modes should be lower in the case of molecules embedded in α -PTCDA than in β -PTCDA crystals. Additionally, a dynamic effect (Davydov splitting) appears as a consequence of the presence of two molecules in the monoclinic unit cell. Due to the in-phase and out-of-phase coupling of vibrations between the two molecules in a unit cell, each internal molecular vibration mode splits into a doublet [12]. The larger FWHM and frequency splitting between the two components resolved for films relative to those obtained for a single phase crystal points to an overlapping of static and dynamic effects caused by a coexistence of both α - and β -PTCDA phases in the films. The decrease in intensity of the higher frequency component, i.e. the 1306.7 cm^{-1} component with increasing temperature, is then consistent with an increase in the content of α -PTCDA at the expense of β -PTCDA phase. Such a behaviour is also supported by the tendency observed for the FWHM of the individual components.

It should be mentioned that another mechanism for the modification of the Raman line shapes may occur, namely the rearrangement of the PTCDA molecules plane with respect to the substrate plane for samples grown at elevated temperatures. In order to clarify the influence of such an effect further investigations using polarized analysis of Raman scattering on samples grown in a larger range of substrate temperatures and with various evaporation rates would be required.

The crystalline domain structure of our films gives rise to significant surface roughness within the lateral spatial range of the laser beam focus ($\sim 6 \times 10^4\text{ }\mu\text{m}^2$). As a consequence, part of the laser

light is diffusely elastically scattered and leads to the background in the low wave number region of the Raman spectra [19,20]. The increase of this background with increasing substrate temperatures indicates an increase in the degree of roughness, corroborating the larger size of individual crystals.

The improvement in crystallinity, i.e. larger size of individual crystals, is also responsible for the increased PL background occurring in the high frequency range of the Raman spectra. A recent study of Gao et al. shows that with increasing substrate growth temperature the crystalline quality of α -naphthylphenylbiphenyl diamide films (800 Å thick) significantly improves [25]. As a consequence, the PL efficiency of NPB films increases markedly. Photoluminescence measurements performed on the PTCDA films revealed an increase of about two orders of magnitude for the sample grown at 410 K with respect to the one grown at 230 K [26].

4.2. X-ray diffraction analysis

The presence of the peak that corresponds to the (1 0 2) lattice planes of the monoclinic system [9,27] in the XRD spectra indicates the existence of crystalline order in all PTCDA films. If one considers the finite crystalline domain size as the main line broadening mechanism, the decrease in the FWHM of the diffraction peak described in the results section reflects the increasing size of the crystalline domains.

The variation of peak position with deposition temperature, on the other hand reveals that crystalline domains of both the α - and β -phases exist [27]. The value of $27.62^\circ (\pm 0.02^\circ)$ for the diffraction angle of films prepared at 360 K and below lies between the theoretical values for the β -phase (27.44°) and the α -phase (27.83°), clearly supporting the coexistence of these phases. The shift of 0.1° for the sample grown at 410 K corroborates the increase in α -phase content already deduced from the Raman line-shape analysis. It should be noticed that the coexistence of the two phases may considerably add to the broadening of the diffraction peak.

The high intensity of the (1 0 2) Bragg diffraction peak for the films grown at 230, 295 and 360 K indicates that within the crystalline domains PTCDA molecules are oriented with their plane (which is approximately parallel to the (1 0 2) lattice plane) parallel to the silicon surface. The decrease of peak intensity for the sample grown at 410 K may be attributed to a change in the molecular orientation relative to the substrate plane in some domains. Möbus and Karl deposited films at even higher temperatures, 520 K, using a higher PTCDA evaporation rate [9]. For that substrate temperature they observed that the peak corresponding to the XRD by (1 0 2) planes vanishes entirely, while a new one corresponding to (0 1 1) planes occurs. This was related to a different growth mechanism with the PTCDA molecular plane approximately upright to the substrate.

5. Summary

PTCDA films with an average thickness of 40 nm were grown on H-passivated Si(1 0 0) by OMBD at four different substrate temperatures: 235, 295, 360, 410 K. At higher temperatures no PTCDA deposition was observed for the evaporation rate of 3 \AA min^{-1} used.

Raman spectra of the films were recorded in situ after the growth was completed. In the spectra of all samples we observe the presence of four external vibrational modes characteristic of the PTCDA molecular crystal. The FWHM of these phonon lines decreases with increasing substrate temperature during deposition. This narrowing mechanism is related, as in the case of the inorganic systems, to an increase of the size of the crystalline domains.

The asymmetric shape of internal vibrational lines is predominantly induced by the presence of α - and β -PTCDA phases in the films. It is also possible that the decrease of FWHM for samples grown at elevated substrate temperatures is affected by an additional rearrangement of PTCDA molecular planes with respect to the substrate plane.

At macroscopic scale, the increase in the size of the crystalline domains leads to a roughening of

the films. This increases the diffusely scattered light background in the low-frequency spectral range for films grown at higher substrate temperature. On the other hand, the formation of larger-size crystallites causes an enhancement of the photoluminescence of PTCDA films, probably through a reduction in nonradiative recombination centres [25].

The XRD spectra of all the films studied displayed the Bragg reflection of the (1 0 2) plane of the PTCDA monoclinic molecular crystal, proving the crystalline structure of films. In good agreement with the Raman results, the FWHM of the (1 0 2) peak decreases with increasing substrate temperature, which mainly reflects the increase in the size of the crystalline domains. A close analysis reveals that the α - and the β -PTCDA coexist within all films. The observed shift towards slightly higher diffraction angles with increasing deposition temperature indicates the increase in the content of the α -phase at the expense of that of the β -phase.

Acknowledgements

This research was supported by the Graduiertenkolleg "Dünne Schichten und nichtkristalline Materialien" at Technische Universität Chemnitz, and by the EU funded Human Potential Research Training Network DIODE (contract no.: HPRN-CT-1999-00164).

References

- [1] S.R. Forrest, *Chem. Rev.* 97 (1997) 1793.
- [2] K. Glöcker, C. Seidel, A. Soukopp, M. Sokolowski, E. Umbach, M. Böhringer, R. Berndt, W.-D. Schneider, *Surf. Sci.* 405 (1) (1998) 1.
- [3] C. Seidel, C. Awater, X.D. Liu, R. Ellerbrake, H. Fuchs, *Surf. Sci.* 371 (1997) 123.
- [4] C. Kendrick, A. Kahn, S.R. Forrest, *Appl. Surf. Sci.* 104–105 (1996) 586.
- [5] Y. Hirose, W. Chen, E.I. Haskal, S.R. Forrest, A. Kahn, *J. Vac. Sci. Technol. B* 12 (1994) 2616.
- [6] T. Bitzer, N.V. Richardson, *Appl. Surf. Sci.* 144–145 (1999) 339.
- [7] W. Mönch, *Semiconductor Surfaces and Interfaces*, Springer, Berlin, 1993.
- [8] V. Le Thanh, D. Bouchier, G. Hincelin, *J. Appl. Phys.* 87 (8) (2000) 3700.
- [9] M. Möbus, N. Karl, *Thin Solid Films* 215 (1992) 213.
- [10] T.U. Kampen, D.A. Tenne, S. Park, G. Salvan, R. Scholz, D.R.T. Zahn, *Phys. Stat. Sol. B* 215 (1999) 431.
- [11] T.U. Kampen, G. Salvan, M. Friedrich, D.A. Tenne, S. Park, D.R.T. Zahn, *Appl. Surf. Sci.* 166 (1–4) (2000) 387.
- [12] D.A. Tenne, S. Park, T.U. Kampen, A. Das, R. Scholz, D.R.T. Zahn, *Phys. Rev. B* 61 (21) (2000) 14564.
- [13] V. Wagner, D. Drews, N. Essers, D.R.T. Zahn, J. Guerts, W. Richter, *J. Appl. Phys.* 75 (11) (1994) 7330.
- [14] H. Fuchigami, S. Tanimura, Y. Uehara, T. Kurata, Sei. Tsunoda, *Jpn. J. Appl. Phys.* 34 (1995) 3852.
- [15] U. Guhathakurta-Ghosh, R. Aroca, *J. Phys. Chem.* 93 (1989) 6125.
- [16] R. Kaiser, M. Freidrich, T. Schmitz-Hübsch, E. Sellam, T.U. Kampen, K. Leo, D.R.T. Zahn, *Fresenius J. Anal. Chem.* 363 (1999) 189.
- [17] R. Scholz, A.Yu. Kobitski, T.U. Kampen, M. Schreiber, D.R.T. Zahn, G. Jungnickel, M. Elstner, Th. Frauenheim, *Phys. Rev. B* 61 (20) (2000) 13659.
- [18] A. Morozov, T.U. Kampen, D.R.T. Zahn, *Surf. Sci.* 446 (3) (2000) 193.
- [19] H. Poulet, J.-P. Matieu, *Spectres de Vibration et Symétrie des Cristaux*, Gordon and Breach, Paris, 1970.
- [20] W. Akemann, A. Otto, H.R. Schober, *Phys. Rev. Lett.* 79 (25) (1997) 5050.
- [21] P.S. Pizani, F. Laniotti, R.G. Jasinevicius, J.G. Duduch, A.J.V. Porto, *J. Appl. Phys.* 87 (3) (2000) 1280.
- [22] R.O. Dillon, J.A. Woolam, V. Katkanant, *Phys. Rev. B* 29 (6) (1984) 3482.
- [23] M.A. Paesler, D.E. Sayers, R. Tsu, J. Gonzales-Hernandez, *Phys. Rev. B* 28 (8) (1982) 4550.
- [24] M. Möbus, N. Karl, T. Kobayashi, *J. Cryst. Growth* 116 (1992) 495.
- [25] Z.Q. Gao, W.Y. Lai, T.C. Wong, C.S. Lee, I. Bello, S.T. Lee, *Appl. Phys. Lett.* 74 (22) (1999) 3269.
- [26] A.Yu. Kobitzki, G. Salvan, T.U. Kampen, H.P. Wagner, D.R.T. Zahn, *Appl. Surf. Sci.*, submitted for publication.
- [27] M. Leonhardt, O. Mager, H. Port, *Chem. Phys. Lett.* 313 (1999) 24.